

Designing Novel Contrast Agents for Magnetic Resonance Imaging. Synthesis and Relaxometric Characterization of three Gadolinium(III) Complexes Based on Functionalized Pyridine-Containing Macrocyclic Ligands

by **Silvio Aime***, **Eliana Gianolio**, and **Davide Corpillo**

Dipartimento di Chimica I.F.M., Università degli Studi di Torino, Via P. Giuria 7, I-10125 Torino

and

Camilla Cavallotti, **Giovanni Palmisano***, and **Massimo Sisti**

Dipartimento di Scienze Chimiche Fisiche e Matematiche, Università degli Studi dell'Insubria, Via Valleggio 11, I-22100 Como

and

Giovanni B. Giovenzana

Dipartimento di Scienze Chimiche Alimentari Farmaceutiche e Farmacologiche, Università degli Studi del Piemonte Orientale "A. Avogadro", Via Bovio 6, I-28100 Novara

and

Roberto Pagliarin

Dipartimento di Chimica Organica e Industriale, Università degli Studi di Milano, Via Venezian 21, I-20133 Milano

The three novel pyridine-containing 12-membered macrocyclic ligands **1–3** were synthesized. The coordinating arms are represented by three acetate moieties in **1** and **3** and by one acetate and two phosphonate moieties in **2**. In all three ligands, the acetate arm in the distal position is substituted, with a benzyl group in **1** and **2** and with an arylmethyl moiety in **3**. The relaxivities r_{1p} (20 MHz, 25°) of Gd^{III} complexes are: **Gd·1**, $r_{1p} = 8.3 \text{ mM}^{-1} \text{ s}^{-1}$; **Gd·2**, $r_{1p} = 8.1 \text{ mM}^{-1} \text{ s}^{-1}$; **Gd·3**, $r_{1p} = 10.5 \text{ mM}^{-1} \text{ s}^{-1}$. ¹H-NMRD and ¹⁷O-NMR T_2 data show that **Gd·1** and **Gd·3** contain two H₂O molecules in the inner sphere, whereas the presence of two phosphonate arms allows the coordination of only one H₂O molecule in **Gd·2**. Interestingly, the exchange lifetime of coordinated H₂O in the three complexes is similar in spite of the difference in the coordination number of the Gd^{III} ion (*i.e.*, 9 in **Gd·1** and **Gd·3**, and 8 in **Gd·2**). ¹H-Relaxometric measurements at different pH and in the presence of lactate and oxalate were carried out to get some insight into the formation of ternary complexes from **Gd·1** and **Gd·3**. Finally, it was found that binding to human-serum albumin (HSA) of **Gd·1** and **Gd·2**, though weak, yields limited relaxivity enhancements, likely as a consequence of effects on the hydration sphere caused by donor atoms on the surface of the protein.

Introduction. – It is well established that the intrinsic contrast in magnetic-resonance images (MRI) can be augmented by the use of contrast agents, which are chemicals able to markedly enhance H₂O protons relaxation rates [1][2]. Most applications of contrast agents has dealt with the use of Gd^{III} complexes because this metal ion couples a large magnetic moment with a long electronic-spin relaxation time. This metal does not possess any physiological function in mammals, and its administration as a free ion is extremely toxic even at low doses (10–20 μmol/kg). For this reason, it is necessary to use ligands that form very stable chelates with Gd^{III} ions [3][4].

The efficacy of a Gd^{III} chelate as MRI contrast agent is usually assessed *in vitro* by measuring its relaxivity, which represents the relaxation enhancement of H_2O protons promoted by the paramagnetic complex at 1 mM concentration. At the magnetic-field strength of clinical tomographs, high relaxivities can be obtained when the Gd^{III} chelate is part of a slowly moving macromolecular system [4]. However, to fully exploit the relaxation enhancement brought about by the long re-orientation time τ_{R} , the Gd^{III} complex must display a short exchange lifetime τ_{M} of the coordinated H_2O molecule(s) [4–6]. Often, τ_{M} is too long and acts as a limiting factor for the attainment of the high relaxivities expected for slowly moving systems. Thus, the first step towards the search for high relaxivities is the identification of a Gd^{III} chelate displaying the best values for the hydration number q and for τ_{M} , because the amplification effect associated with the formation of a macromolecular adduct strictly depends on the relaxometric properties of the free complex.

Gd^{III} Chelates with $q = 2$ have often been addressed, as these may represent a good compromise between high hydration and sufficiently high thermodynamic stability. Moreover, the presence of two H_2O molecules in the inner coordination sphere is expected to endow such systems with a faster H_2O exchange than that found with complexes of octacoordinating ligands [7][8]. With regard to this, $[\text{Gd}(\text{DO3A})]$ (Fig. 1) and several of its functionalized derivatives have been investigated in depth [9]. The main drawback found with this structural type lies in a relaxivity ‘quenching’ effect upon interacting with proteins, as donor atoms of Asp or Glu residues may replace the coordinated H_2O molecules. It has been suggested that the occurrence of such interactions can be anticipated by investigating the formation of ternary complexes between a given complex and substrates like lactate, malonate, or, simply, carbonate [10].

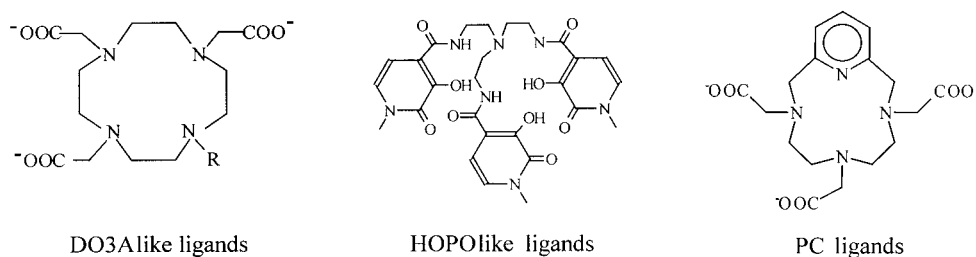


Fig. 1. Three classes of heptadentate ligands: DO3A, HOPO, and PC ligands

Whereas $[\text{Gd}(\text{DO3A})]$ -like complexes show quite strong interactions with the latter substrates, it has been found that two other classes of heptacoordinated Gd^{III} chelates ($q = 2$) do not. The first class is represented by $[\text{Gd}(\text{HOPO})]$ complexes developed by Raymond and co-workers [11–13]. The second class is represented by Gd^{III} complexes with ligands based on a 12-membered N_4 pyridine-containing macrocycle (PC-type ligands) in which the three amino N-atoms bear acetic or phosphonic arms (Fig. 1) [14–16].

Among the Gd^{III} complexes with PC-type ligands, we have recently identified $[\text{Gd}(\text{PCP2A})]$ (PCP2A = pyridine-containing macrocycle (PC) bearing two acetate (A) and one methylenephosphonate (P) arms) as a very promising contrast agent for improved applications in MRI [17]. It shows a very high stability constant ($\log K_{\text{F}} = 23.4$) and a relaxivity *ca.* two times higher than the values reported for contrast agents

currently used in clinical practice. Moreover, [Gd(PCP2A)] displays a fast exchange of the coordinated H₂O molecules.

The results now presented deal with Gd^{III} complexes of modified PC-type ligands and are aimed at assessing the effects on the observed relaxivity arising from the presence of an aromatic substituent at the distal arm and from the replacement of acetate for phosphonate arms at the two equivalent N-atoms. The structures of the three novel PC-type ligands **1–3** synthesized in this work are shown in *Fig. 2*.

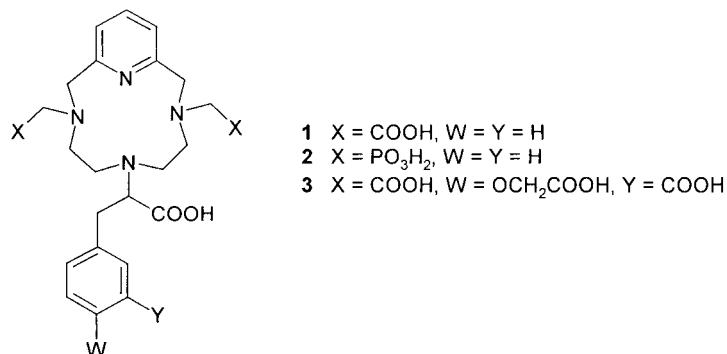


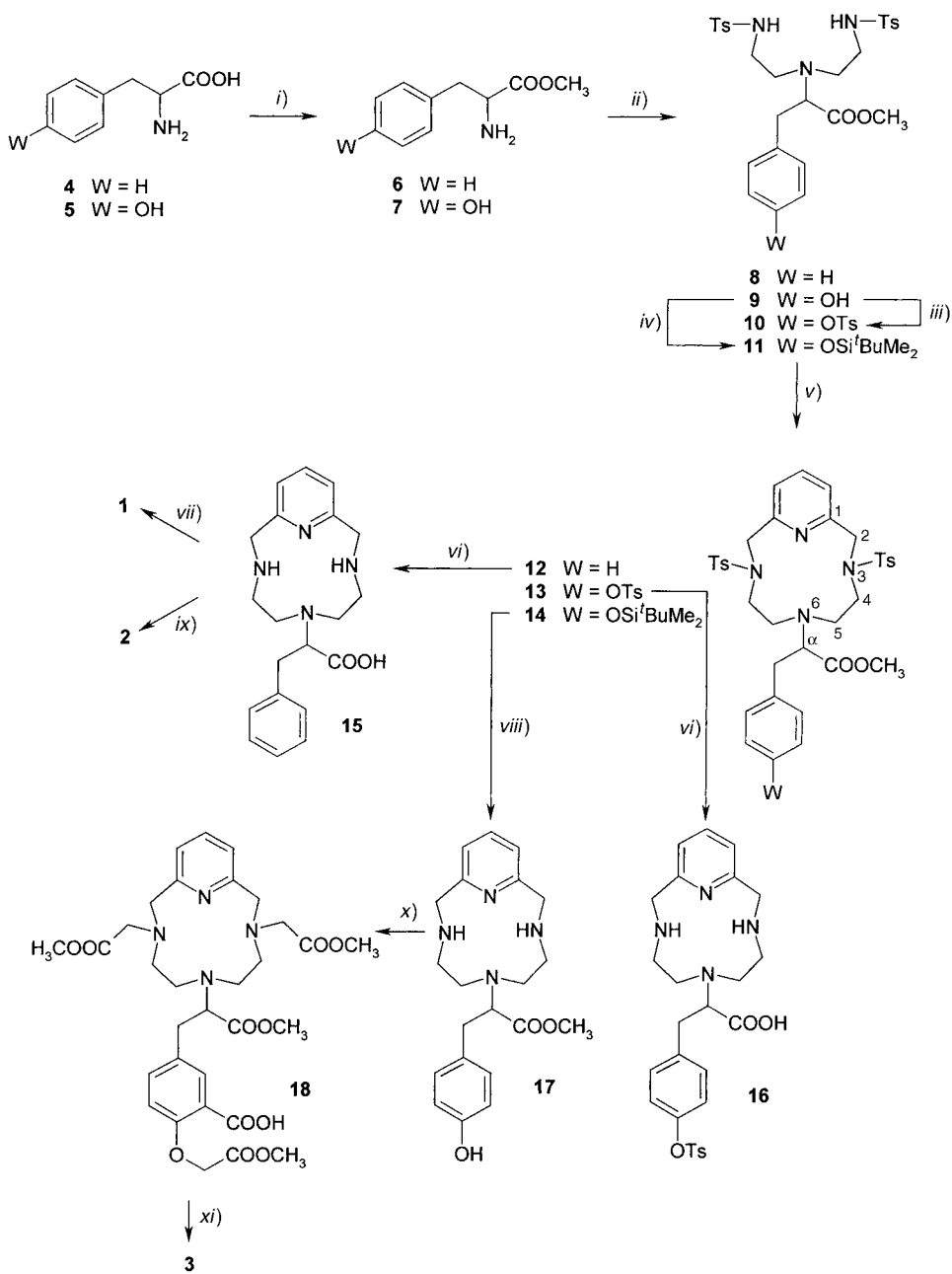
Fig. 2. PC-Type ligands **1–3**

Results and Discussion. – *Synthesis of Ligands 1–3 (Scheme 1).* The strategy we envisioned for the synthesis of **1–3** was essentially based on the nucleophilic ring opening of 1-tosylaziridines by the appropriate α -amino esters to afford centrally *N*-functionalized diethylenetriamines. This approach proved to be highly efficient in the synthesis of diethylenetriamine derivatives, and it is well documented in the literature [17]. As already reported by us [15], these compounds, where the tosyl moieties act as protecting-activating groups, are reactive nucleophiles allowing ring cyclization with 2,6-bis(halomethyl)pyridine under appropriate experimental conditions.

Thus, the commercially available α -amino acids L-phenylalanine (**4**) and L-tyrosine (**5**) were transformed into the corresponding methyl esters by treatment with thionyl chloride in MeOH at 0°. The reactivity of the two ester derivatives **6** and **7** towards 1-tosylaziridine (obtained by standard methods from ‘*N,O*-ditosylethanolamine’ = 2-[[[(4-methylphenyl)sulfonyl]amino]ethyl 4-methylbenzenesulfonate]) proved to be similar: the ring opening of 1-tosylaziridine (2.2 equiv./equiv. ester) took place in refluxing toluene affording the two functionalized diethylenetriamines **8** and **9** in excellent yields (90%) after silica-gel chromatography.

The evaluation of these centrally *N*-functionalized derivatives in macrocyclization reactions was first performed with compound **8**. By reacting **8** with 2,6-bis(chloromethyl)pyridine in refluxing anhydrous MeCN in the presence of anhydrous K₂CO₃, the macrocycle **12** was obtained in 65% yield after crystallization. The experimental conditions we adopted here represent a modification of the *Richman–Atkins* protocol. We already observed [15] that higher yield in PCTA (pyridine-containing macrocycle triacetate) derivatives may be obtained by performing the macrocyclization step under heterogeneous conditions as reported above. Indeed, under *Richman–Atkins* conditions

Scheme. Synthesis of Ligands 1–3



i) MeOH, SOCl₂, 0°. ii) 1-Tosylaziridine, toluene, reflux. iii) TsCl, Py, 0°. iv) ^tBuMe₂SiCl, ⁱPr₂EtN, MeCN, 0°. v) 2,6-Bis(chloromethyl)pyridine, anh. K₂CO₃, MeCN, reflux. vi) 48% aq. HBr, PhOH, AcOH, reflux. vii) ClCH₂COOH, KOH, H₂O, 80°. viii) 30% HBr in AcOH, 60°. ix) H₃PO₃, (CH₂O)_n, 6M aq. HCl, reflux. x) BrCH₂COOMe, Ag₂CO₃, MeCN, r.t. xi) KOH, MeOH, 60°.

(NaH/DMF as base/solvent system), compound **12** was isolated in less than 30% yield. Removal of the protecting-activating tosyl groups and hydrolysis of the methyl ester moiety to give the macrocyclic polyamino acid **15** was accomplished by refluxing **12** with 48% aqueous HBr in AcOH in the presence of phenol as tosyl scavenger.

The macrocyclic amino acid **15** represents the key intermediate for the preparation of ligands **1** and **2**. Thus, alkylation of **15** with chloroacetic acid in the presence of KOH at 80° at pH *ca.* 10, followed by treatment with conc. HCl solution at room temperature (pH 0) and chromatography (*XAD 1600*) gave pure **1** in 68% yield. The introduction of the two phosphonomethyl substituents at the two NH moieties of **15** was accomplished by reaction with H₃PO₃ and CH₂O in 6M HCl under reflux, affording pure **2** in 61% yield after precipitation by EtOH.

The reaction of diethylenetriamino **9** with 2,6-bis(chloromethyl)pyridine in refluxing MeCN in the presence of K₂CO₃ afforded polymeric materials as the only products. Likely, the lability of the phenolic OH group towards oxidation is responsible for the failure of the macrocyclization step. However, upon protecting the OH group of **9** as tosyl (\rightarrow **10**) or (*tert*-butyl)dimethylsilyl ether derivatives (\rightarrow **11**), we were able to observe the formation of the desired macrocycles **13** (60%) and **14** (62%), respectively, in the reaction with 2,6-bis(chloromethyl)pyridine under heterogeneous conditions. Treatment of **13** with aqueous HBr solution, AcOH, and phenol removed the *N*-tosyl groups while the phenolic tosylate moiety remained unaffected (\rightarrow **16**). However, when compound **16** was subjected to alkaline hydrolysis (KOH in H₂O, MeOH, glyme, PEG), no reaction was observed at room temperature, and, at higher temperature, extensive decomposition took place. The removal of the protecting groups of **14** proved more successful. By reacting **14** with anhydrous 33% HBr in AcOH, compound **17** was obtained in almost quantitative yield. Surprisingly, the methyl ester moiety remained unaffected under these conditions. The use of 48% aqueous HBr, which worked well with **12**, afforded lower yields of **17**. Attempted alkylation of **17** with chloroacetic acid in H₂O (pH 10) produced only a complex reaction mixture in which the desired product could not be identified. The ease of oxidation of the phenolic OH group could be responsible for the failure of this reaction. No success was met with also for the reaction of **17** with *tert*-butyl bromoacetate in various solvents (MeCN, DMF) and in the presence of different bases (K₂CO₃, Et₃N, ⁱPr₂EtN). However, by reacting **17** with methyl bromoacetate in the presence of Ag₂CO₃ and in the dark, compound **18** was obtained in 58% yield. NMR and MS analyses confirmed the structure of **18**, which likely derives from a *Kolbe*-like carboxylation side reaction, followed by normal peralkylation. Finally, alkaline hydrolysis of **18** (KOH/MeOH, reflux) afforded ligand **3**.

Synthesis and Relaxometric Characterization of Gadolinium(III) Complexes with Ligands 1–3. The Gd^{III} complexes of ligands **1–3** were synthesized by adding stoichiometric amounts of GdCl₃ to aqueous solutions of the ligands while maintaining neutral pH with 1M NaOH. Formation of the complex was followed by measuring the H₂O proton relaxation rate on a relaxometer operating at 20 MHz.

The relaxivities r_{1p} of **Gd·1**, **Gd·2**, and **Gd·3**, measured at 20 MHz and 25°, are 8.3, 8.1, and 10.5 mm⁻¹ s⁻¹ respectively. In *Fig. 3*, a plot of the relaxivities of these complexes and of previously reported ones based on heptadentate ligands, as a function of the molecular mass is reported. The relaxivities of the complexes **Gd·1**, **Gd·2**, and **Gd·3** are in the range of expected values for similarly sized complexes with $q = 2$.

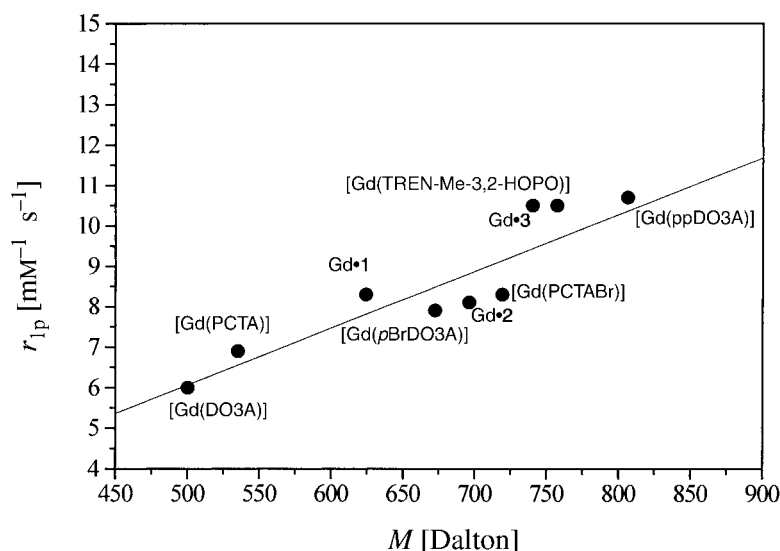


Fig. 3. Relaxivities (measured at 0.47 T, pH 7, and 25°) of some Gd^{III} complexes with $q = 2$ as a function of their molecular mass

More insight into the parameters involved in paramagnetic relaxation pathways and into the effective hydration state were obtained by measuring the $1/T_1$ NMRD profiles over an extended observation frequencies range at 25° (Fig. 4, a–c). Experimental data were fitted considering that the observed relaxivity is given by the sum of four contributions shown in Eqn. 1 [18], where R_{1d} represents the diamagnetic contribution of pure H_2O protons (0.38 s^{-1}), R_{1p}^{is} is given by the contribution of the inner-sphere H_2O molecule(s) directly coordinated to the metal ion, R_{1p}^{2nd} arises from the second-sphere H_2O molecules, and R_{1p}^{os} deals with the contribution of H_2O molecules that diffuse in the proximity of the paramagnetic complex. The latter contribution, for small Gd^{III} complexes, may be considered to be a constant value, *i.e.*, *ca.* $2.3\text{--}2.5 \text{ mM}^{-1} \text{ s}^{-1}$ at 25° and 20 MHz [5].

$$R_1^{\text{obs}} = R_{1d} + R_{1p}^{\text{is}} + R_{1p}^{\text{2nd}} + R_{1p}^{\text{os}} \quad (1)$$

The inner- and the second-sphere relaxivities may be evaluated on the basis of the set of equations derived from the Solomon–Bloembergen–Morgan (SBM) theory (Eqns. 2–4) [19][20], where q is the number of inner- or second-sphere H_2O molecules, T_{1M} is the longitudinal relaxation time of their protons, r is the Gd–H distance, τ_R is the molecular re-orientation time, τ_M is the coordinated- H_2O exchange lifetime, and τ_S is the electronic relaxation time.

$$R_{1p} = \frac{q}{55.5(T_{1M} + \tau_M)} \quad (2)$$

$$(T_{1M})^{-1} \propto \frac{K}{r^6} f(\tau_C) \quad (3)$$

$$(\tau_C)^{-1} = (\tau_S)^{-1} + (\tau_M)^{-1} + (\tau_R)^{-1} \quad (4)$$

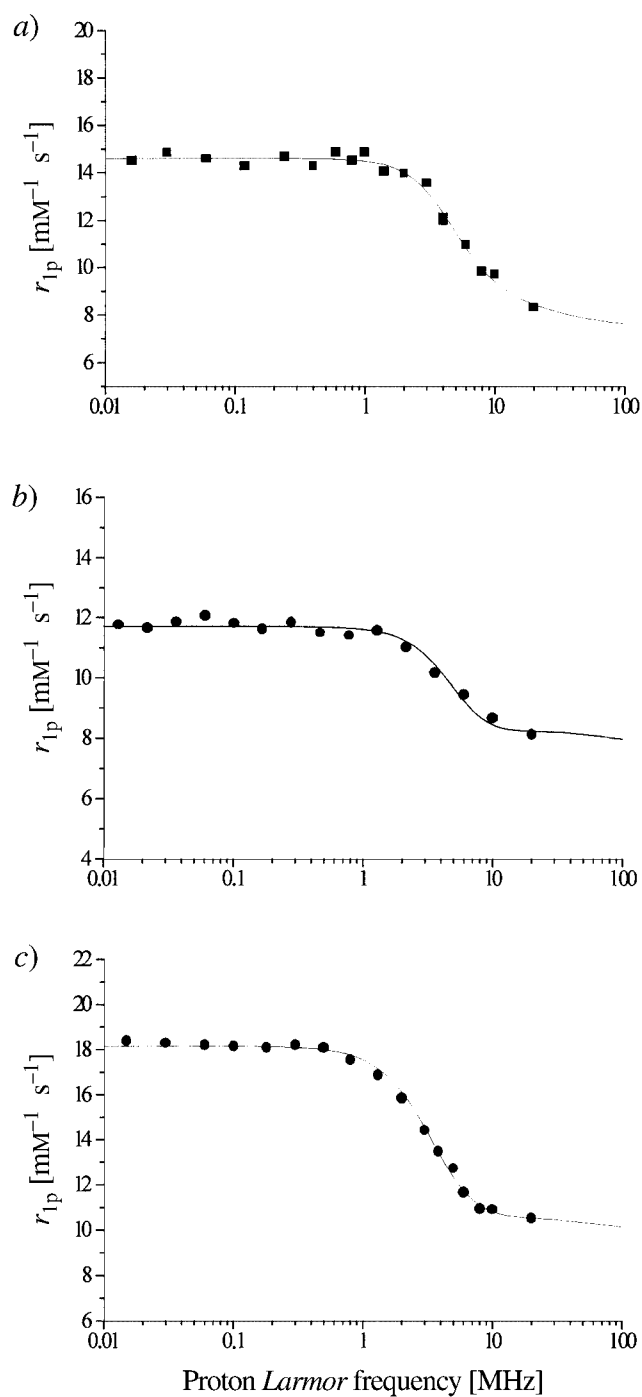


Fig. 4. $1/T_1$ NMRD profiles of a 1 mM solution of a) **Gd-1**, b) **Gd-2**, and c) **Gd-3** at pH 7 and 25°. The solid curves through the data points were calculated by means of the parameters reported in the Table.

The best fit of the experimental data was obtained by considering two coordinated H₂O molecules for **Gd·1** and **Gd·3** and only one inner-sphere H₂O molecule for **Gd·2**. The relatively high relaxivity featuring **Gd·2** is due, besides the inner-sphere contribution, to the presence of two second-sphere H₂O molecules at a distance of 3.8 Å from the Gd^{III} ion. The occurrence of two second-sphere H₂O molecules was surmised on the basis of a comparison with the previously reported results on the parent chelate [Gd(PCP2A)(H₂O)₂] [17]. In the latter complex, the observed R_{1p} value (8.3 mm⁻¹ s⁻¹) was justified on the basis of the presence of two inner-sphere and one second-sphere H₂O molecules. Passing from [Gd(PCP2A)(H₂O)₂] to **Gd·2**, one may expect that the presence of two phosphonate groups yields either a decrease of the number of directly coordinated H₂O molecules (from two to one) and an increase of the number of H₂O molecules in the second coordination sphere (from one to two). The results from the best-fit procedure were fully consistent with this expectation. The relaxometric parameters determined by fitting the NMRD experimental data to *Eqns. 1–4* for the three complexes (see *Table*) are similar to those reported for related complexes derived from PCTA-like ligands.

Table. *Best-Fit Parameters Obtained from the Analysis of the NMRD and ¹⁷O-NMR Profiles Considering a Metal–H Distance of 3.1 Å for the Inner-Sphere H₂O Molecules and 3.8 Å for the Second-Sphere Water, and a Metal–O Distance of 2.5 Å. Δ^2 = mean-square zero-field energy, τ_v = correlation time for the modulation of the zero-field-splitting interaction, τ_R = molecular re-orientation time; τ_M = exchange lifetime of coordinated H₂O; q = hydration number of inner sphere; q^{2nd} = hydration number of second sphere.*

	Δ^2 [10 ¹⁹ s ⁻²]	τ_v [ps]	τ_R [ps]	τ_M [ns]	q	q^{2nd}
Gd·1	1.98	36	92	58	2	0
Gd·2	3.7	27	120	75	1	2
Gd·3	2.2	27	134	79	2	0
Gd·3 (pH 10)	1.02	39	130	180	1	0

It is interesting to note that while the substitution of one coordinating acetate arm (A) with a phosphonate one (P), as in the case of [Gd(PCP2A)] [17], does not cause reduction of the hydration state, the hindrance caused by the introduction of two phosphonate groups (see **Gd·2**) leads to the formation of a complex with $q = 1$ as in the case of [Gd(PCTP)] [12] which contains three phosphonate moieties [9]. Thus, the progressive replacement of the acetate arms with phosphonate ones causes a reduction in hydration state of the metal ion analogously to what was observed on going from DOTA (= DO3A; see *Fig. 1*) to DOTP Ln^{III} complexes [21].

To determine the exchange lifetime of the coordinated H₂O molecules in the three Gd^{III} complexes, we measured their ¹⁷O-NMR transverse relaxation time as a function of temperature (*Fig. 5, a–c*) [22]. According to the *Swift-Connick* theory [23], the paramagnetic contribution (R_{2p}^O) to the observed transversal relaxation rate is given by *Eqn. 5*, and the temperature dependence of $\Delta\omega_M^O$ is described by *Eqn. 6*, where B_0 is the magnetic-field strength, and A/\hbar is the Gd,¹⁷O scalar coupling constant (whose value for (polyaminocarboxylato)gadolinium(III) complexes has been fixed to $-3.8 \cdot 10^6$ rad s⁻¹) [18]. For relatively small-sized Gd^{III} chelates and at 2.1 T, R_{2M}^O is essentially dominated by the electron-nucleus scalar interaction (see *Eqns. 7 and 8*), and, finally, the temperature dependence of R_{2p}^O is expressed in terms of the *Eyring* relationship for

τ_M and τ_ν according to Eqn. 9, where j refers to the two different dynamic processes involved ($j = \nu, M$) and ΔH_j is the corresponding activation enthalpy.

$$R_{2p}^O = \frac{qC}{55.6} \tau_M^{-1} \frac{R_{2M}^{O^2} + \tau_M^{-1} R_{2M}^O + \Delta\omega_M^{O^2}}{(R_{2M}^O + \tau_M^{-1})^2 + \Delta\omega_M^{O^2}} \quad (5)$$

$$\Delta\omega_M^O = \frac{g_e \mu_B S(S+1) B_0}{3k_B T} \frac{A}{\hbar} \quad (6)$$

$$R_{2M}^O = \frac{1}{3} \left(\frac{A}{\hbar} \right)^2 S(S+1) \left(\tau_{E1} + \frac{\tau_{E2}}{1 + \omega_s^2 \tau_{E2}^2} \right) \quad (7)$$

$$\tau_{Ei}^{-1} = T_{iE}^{-1} + \tau M^{-1} \quad (8)$$

$$(\tau_j)_T^{-1} = \frac{(\tau_j^{-1})^{298.15} T}{298.15} \exp \left[\frac{\Delta H_j}{R} \left(\frac{1}{298.15} - \frac{1}{T} \right) \right] \quad (9)$$

In Fig. 5, a–c, the variable-temperature ^{17}O -NMR profiles of the three complexes are reported; all of them show the typical behavior of fast-exchange conditions, since R_{2p} steadily decreases as the temperature increases. The exchange lifetimes τ_M determined at 298 K (Table) are very similar. This is a surprising result, as we would have expected different τ_M values for **Gd·1** and **Gd·2** because the difference in their coordination number might suggest that two different exchange mechanisms are operating. In fact, the Gd^{III} ion in complex **1** has a coordination number 9; therefore, the mechanism operating the exchange of the coordinated H_2O molecules should be a dissociative one. On the other hand, the coordination number of the Gd^{III} ion in complex **2** is 8, and we expect the occurrence of an associative mechanism. Although it has been assessed that the H_2O -exchange rate may depend upon several factors, it was early established that the very fast exchange observed for octacoordinate complexes (such as the aqua ion $[\text{Gd}(\text{H}_2\text{O})_8]^{3+}$ or $[\text{Gd}(\text{PDTA})]$) occurs by an associative mechanism involving a nonacoordinate transition state [24][25][9]. Likely, the enthalpy of the $\text{Gd}-\text{OH}_2$ bond is the rate-determining parameter for both complexes.

The coordination geometry in **Gd·2** is a square antiprism whose eight coordination sites are taken by the four N-atoms (lower N_4 plane) and by two phosphonate O-atoms, one acetate O-atom, and one H_2O O-atom (upper O_4 plane) [3]. Each phosphonate group keeps one H_2O molecule in the second coordination sphere. One may envisage a possible exchange pathway that, after the dissociation of the coordinated H_2O , delivers the second-sphere H_2O into the inner coordination sphere. In principle, such a mechanism might have some analogy with that operating in **Gd·1**. One may envisage that the rate-determining step in the exchange path occurring in the latter complex is the dissociation of the H_2O molecule in the O_4 plane, whose vacancy is then occupied by the H_2O that is in the capping position.

Formation of Ternary Complexes. The study of the pH effect on the relaxivity of a Gd^{III} complex may provide several relevant information. In the acid limb, increase of r_1 may report the protonation of ligand functionalities, which may change the hydration

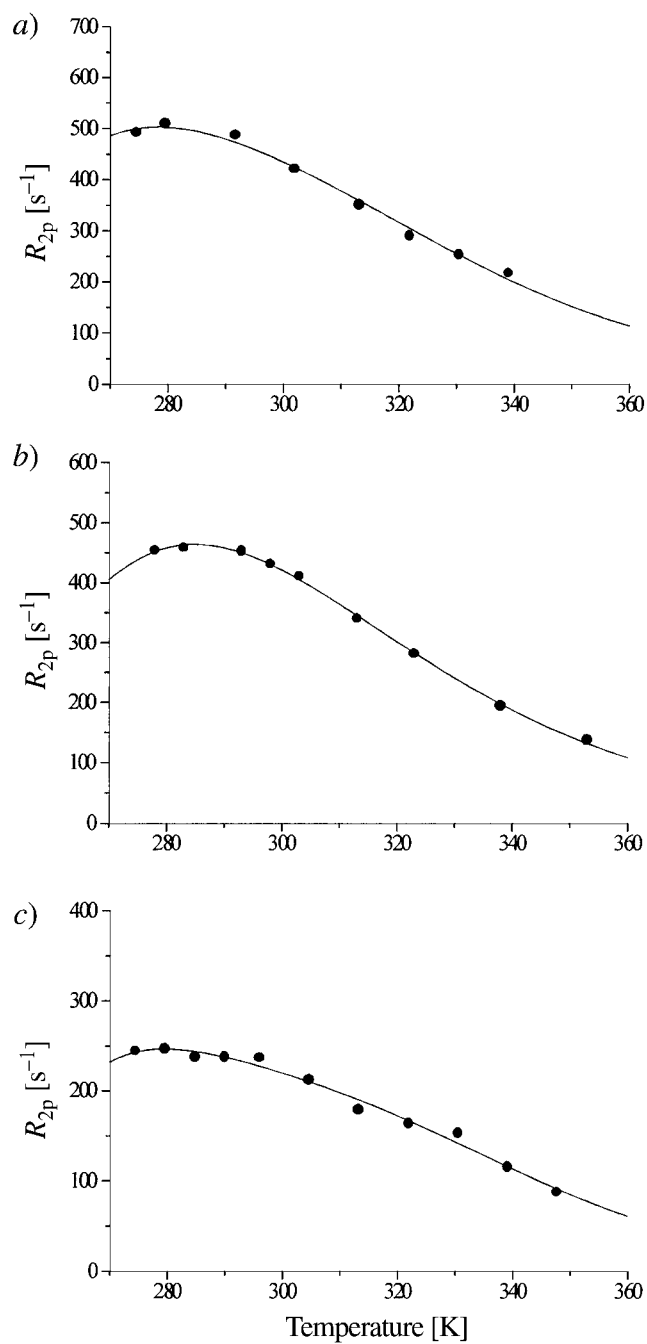


Fig. 5. Temperature dependence of the transverse water relaxation rate (R_{2p}) for a 20 mM solution of a) **Gd-1** (2.1 T, pH 7), b) **Gd-2** (7 T, pH 7), and c) **Gd-3** (2.1 T, pH 7)

state or even may cause the release of Gd^{III} ions. In the basic limb, a decrease in relaxivity may be an indication of the formation of ternary complexes with the carbonate anion [26][9]. The latter condition is often met with heptacoordinate complexes, and it is a clue to the possible formation of ternary complexes in the presence of other O-donor substrates [27].

In *Fig. 6*, the plots of r_1 values as function of the solution pH for the three complexes are reported. All three complexes are very stable at acid pH, as expected on the basis of very high K_f values previously reported for $[\text{Gd}(\text{PCTA})]$ [16] and $[\text{Gd}(\text{PCP2A})]$ [17]. At the basic limb, only **Gd·2** maintains a constant r_{1p} , whereas **Gd·1** and **Gd·3** show similar decreases in r_1 , characteristic of the formation of an adduct with carbonate ions. To get more insight into the structural and dynamic properties of the ternary complex with carbonate anion, the $1/T_1$ NMRD profile of **Gd·3** at pH 10 was recorded (*Fig. 7*). The fit of the experimental data to the values calculated on the basis of *SBM* theory are reported in the *Table*. From this analysis, it was found that, in the ternary complex, the carbonate ion replaces only one H_2O molecule. The remaining inner-sphere H_2O molecule displays a τ_M value of 180 ns as assessed by ^{17}O -NMR R_2 measurements at variable temperature. This value is in accord with other macrocyclic-based systems with $q=1$ derived from DOTA (=DO3A; see *Fig. 1*). On this basis, we may tentatively suggest that there is a direct correspondence between the two structures drawing the conclusion that the carbonate O-atom coordinates the Gd^{III} ion at a corner position of the upper O_4 plane. Therefore, the H_2O molecule in the **Gd·3**/carbonate system occupies an apical position. The observed elongation of τ_M in the ternary complex supports the view forwarded in the previous section that a H_2O molecule coordinated in the O_4 plane is responsible for the faster exchange detected for **Gd·1** and **Gd·3**.

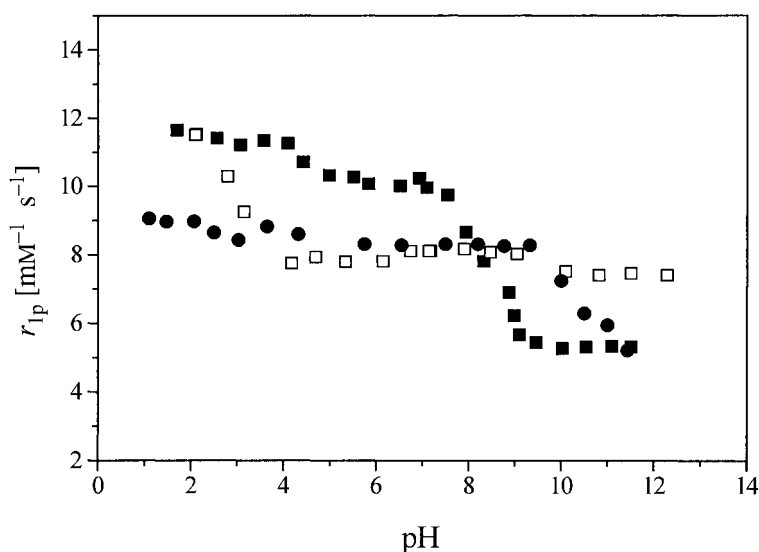


Fig. 6. pH Dependence of the proton relaxivity (r_{1p}) of **Gd·1** (●), **Gd·2** (□), and **Gd·3** (■) measured at 0.47 T and 25°

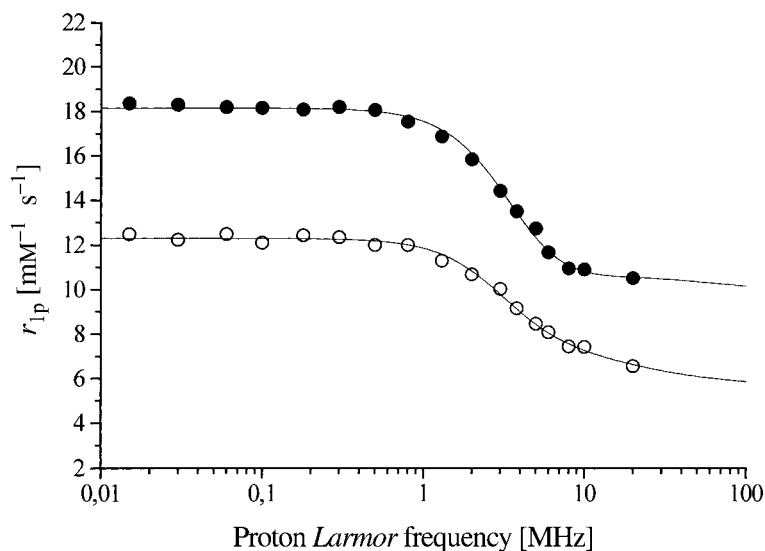


Fig. 7. $1/T_1$ NMRD Profiles of a 1 mM solution of **Gd·3** at pH 7 (●) and pH 10 (○) and 25°. The solid curves through the data points were calculated with the parameters reported in the Table.

The pH dependence anticipates the results obtained by monitoring the changes in r_1 upon addition of increasing amounts of O-donor substrates like lactate, oxalate, and tartrate. In fact, only **Gd·1** and **Gd·3** show a decrease of r_1 upon addition of the substrates, whereas r_1 of **Gd·2** is unaffected. The different behavior clearly reflects the hydration state of the three complexes: when $q = 1$, no formation of ternary adduct is detected, whereas, when $q = 2$, a bidentate ligand can replace the two inner-sphere H_2O molecules. The binding affinity towards lactate is rather low for **Gd·1** ($K_a = 16 \text{ M}^{-1}$) and similar to the value found for the parent [Gd(PCTA)] complex ($K_a = 22 \text{ M}^{-1}$), while it is higher for **Gd·3** ($K_a = 188 \text{ M}^{-1}$). The presence of two negative charges in **Gd·3** does not hamper lactate binding. Actually, the increased affinity of **Gd·3** for this ligand may reflect minor structural changes on the inner coordination cage caused by the outer substituent.

A much stronger binding affinity was observed for the oxalate ligand ($K_a = 382 \text{ M}^{-1}$ for **Gd·1** and $K_a = 2.4 \cdot 10^5 \text{ M}^{-1}$ for **Gd·3**). Again **Gd·3**, in spite of the residual negative charge, shows a stronger affinity for the entering substrate.

Binding to Macromolecules. As anticipated in the introduction, the attainment of high relaxivities is pursued through the binding of the Gd^{III} chelate to a macromolecular system. An approach that has met with a large success consists of forming noncovalent adducts between a suitably functionalized Gd^{III} complex and human-serum albumin (HSA) [5][28][29]. Although the substituents present on the surface of the complexes **Gd·1**, **Gd·2**, and **Gd·3** were not designed for this specific purpose, we investigated their affinity for HSA.

The assessment of the HSA-binding capability of a given Gd^{III} complex is conveniently carried out *in vitro* by means of the proton relaxation enhancement (PRE) method. In this method, by titrating a solution of the paramagnetic complex

with a concentrated solution of HSA, it is possible to determine the thermodynamic binding constant (K_a) and the relaxivity of the macromolecular adduct (r_1^b) [27]. This method is based on the measurement of the increase in the H_2O proton longitudinal relaxation rate that take place when a paramagnetic complex binds to a slowly tumbling macromolecule as a consequence of the elongation of its τ_R value. **Gd·1** binds very weakly ($K_a = 200 M^{-1}$), yielding an estimated value for the relaxivity of the all-bound adduct of *ca.* $40 \text{ mM}^{-1}\text{s}^{-1}$. **Gd·2** binds more tightly ($K_a = 3300 M^{-1}$), but the attainable relaxivity for the paramagnetic macromolecular adduct is significantly smaller ($r_1^b = 24.4 \text{ mM}^{-1}\text{s}^{-1}$). **Gd·3** does not interact at all with HSA. The observed behavior can be accounted for in terms of the following assumptions: *i*) The phosphonate groups contribute to the binding (as previously established for [Gd(DOTP)] and [Gd(PCTP)] [30]), but the geometry at the interacting site is such that either the inner-sphere H_2O molecule exchange is made much more difficult, or the H_2O is excluded by direct coordination of protein donor atoms to the paramagnetic center. The relaxivity found for the all-bound **Gd·2** adduct is similar to that observed for the [Gd(DOTP)]/HSA adduct where only second-sphere and outer-sphere contributions are operating. *ii*) On comparing the binding affinities of **Gd·1** and **Gd·2**, one draws the conclusion that the benzyl moiety is definitively inadequate to promote hydrophobic binding. *iii*) The presence of two negative charges at the aromatic substituent in **Gd·3** further reduces the binding towards HSA, *i.e.*, the system becomes too hydrophilic for yielding any measurable binding to the protein.

The estimate of a relaxivity of $40 \text{ mM}^{-1}\text{s}^{-1}$ for the **Gd·1**/HSA adduct appears lower than expected for the characteristics of this complex. Likely, decreased hydration takes place upon binding to the protein. Thus, the binding through the benzylic moiety at the distal arm appears unable to avoid the interference of the protein with the H_2O coordinated to the Gd^{III} center. Suitable functionalization should involve large-sized groups able to keep the chelate moiety sufficiently far apart from the protein surface.

To get some support for this hypothesis, we carried out analogous measurements in the presence of poly- β -cyclodextrin (poly- β -CD, polymerization degree = 12), which has been previously shown to be a good model for the formation of macromolecular adducts based on simple hydrophobic interactions [31]. The binding of **Gd·1** and **Gd·2** with poly- β -CD yielded K_a values of 300 and $95 M^{-1}$, respectively. Interestingly, the relaxation enhancements measured for the two adducts are significantly higher than those found in the case of the corresponding adducts with HSA, being *ca.* 57 and $46 \text{ mM}^{-1}\text{s}^{-1}$ for **Gd·1** and **Gd·2**, respectively. The binding affinity of **Gd·3** towards poly- β -CD is very small ($K_a = 15 M^{-1}$), and the calculation of the relaxivity of the all-bound system is more subject to error. Within these limits, we estimate a value for the macromolecular adduct of $68 \text{ mM}^{-1}\text{s}^{-1}$. Thus, the results from the analysis of the relaxometric titration with poly- β -CD clearly indicate that very high relaxivities can be obtained upon the formation of macromolecular adducts provided that the macromolecule itself has no 'quenching' effect on the hydration properties of the paramagnetic agent.

Conclusions. – In summary, it is worth to highlight the main conclusions we draw from the results obtained in this work: *i*) In agreement with previous observations [9][17], the presence of two coordinating phosphonate groups causes a decrease in the

number of the inner-sphere H₂O molecules. The effect on the observed relaxivity is compensated by the ability of phosphonate moieties to increase the second hydration sphere of the complex.

ii) The rule that Gd^{III} complexes with coordination number 9 should show a slower exchange rate of the coordinated H₂O with respect to systems endowed with coordination number 8 is not confirmed here. Indeed, ¹⁷O-NMR *T*₂ data unambiguously show that τ_M of the coordinated H₂O in **Gd·1** and **Gd·2** are very similar in spite of the change in coordination number.

iii) The active role of HSA on the hydration properties of **Gd·1** and **Gd·2** indicates that the benzyl moiety, although bonded to the distal acetate arm, is unable to keep the coordination cage sufficiently inert to attack of donor atoms present on the surface of the protein. Likely, larger-sized groups have to be used to avoid such behavior, which largely ‘quenches’ the attainable relaxivity enhancement.

Experimental Part

1. *General.* All chemicals were purchased from *Aldrich* and used without further purification. Anal. TLC: silica gel 60F₂₅₄ (*Macherey-Nagel*), detection by spraying with *Dragendorff* reagent. M.p.: uncorrected; *Büchi-510* apparatus. ¹H- and ¹³C-NMR Spectra: at 200 and 50.3 MHz, resp.; *Bruker AC-200* spectrometer; CDCl₃ soln., unless stated otherwise; chemical shifts δ in ppm downfield from internal SiMe₄ (=0.00 ppm), *J* in Hz. Mass spectra: ESI-ion trap (*Bruker Esquire 3000 Plus*) or MALDI-TOF (*Bruker Reflex III* spectrometer) in *m/z*. Elemental analyses: *Perkin-Elmer 240* instrument.

2. *Esterification: General Procedure.* To a suspension of L-amino acid **4** or **5** (60.0 mmol) in MeOH (80 ml) at 0°, SOCl₂ (9.0 ml) is slowly added. The obtained soln. is stirred at r.t. for ca. 2.5 h and is then heated at 40° for 1 h. The solvent is evaporated. To the oily residue, 10% aq. Na₂CO₃ soln. is added and the suspension extracted with AcOEt (3 × 30 ml). The org. phase is dried (Na₂SO₄) and evaporated to give pure **6** and **7**, resp.

L-Phenylalanine Methyl Ester (**6**): Colorless oil (8.6 g, 80%). ¹H-NMR: 7.23–7.10 (*m*, 5 H); 3.62–3.54 (*m*, 4 H); 3.00 (*m*, 1 H); 2.80 (*dd*, *J* = 12.4, 7.2, 1 H); 1.42 (*br. s*, 2 H). ¹³C-NMR: 172.2 (C); 137.1 (C); 129.1 (CH); 128.4 (CH); 126.6 (CH); 55.6 (CH); 51.7 (Me); 41.0 (CH₂).

L-Tyrosine Methyl Ester (**7**): Light yellow solid (9.4 g, 80%). M.p. 134–135°. ¹H-NMR: 6.87, 6.65 (*AA'BB'*, *J* = 8.1, 4 H); 3.59–3.53 (*m*, 4 H); 2.87 (*dd*, *J* = 13.6, 4.7, 1 H); 2.62 (*br. s*, 3 H); 2.67 (*dd*, *J* = 13.6, 7.6, 1 H). ¹³C-NMR: 175.3 (C); 156.1 (C); 130.1 (CH); 127.4 (C); 115.5 (CH); 55.8 (CH); 51.8 (Me); 40.1 (CH₂).

3. *Reaction with 1-Tosylaziridine: General Procedure.* The appropriate amino acid methyl ester **6** or **7** (20 mmol) and 1-tosylaziridine (44 mmol) are dissolved in toluene (20 ml) and the soln. refluxed for 6 h. The solvent is then evaporated and the waxy solid purified by FC (silica gel; for **8**, hexane/*i*PrOH 9:1; for **9**, hexane/*i*PrOH/CH₂Cl₂ 9:0.5:0.5).

N,N-Bis[2-[(4-methylphenyl)sulfonyl]amino]ethyl]-L-phenylalanine Methyl Ester (**8**). Yellow waxy solid (10.3 g, 90%). ¹H-NMR: 7.71, 7.27 (*AA'BB'*, *J* = 8.2, 8 H); 7.23–7.12 (*m*, 5 H); 5.11 (*br. s*, 2 H); 3.59 (*s*, 3 H); 3.43 (*t*, *J* = 7.4, 1 H); 2.97 (*dd*, *J* = 14.1, 7.4, 1 H); 2.85–2.60 (*m*, 9 H); 2.39 (*s*, 6 H). ¹³C-NMR: 172.3 (C); 143.2 (C); 138.0 (C); 136.7 (C); 129.6 (CH); 129.1 (CH); 128.6 (CH); 127.0 (CH); 126.6 (CH); 64.4 (CH); 51.4 (Me); 50.5 (CH₂); 40.8 (CH₂); 35.6 (CH₂); 21.4 (Me). ESI-MS: 574 ([*M* + H]⁺), 1147 ([2*M* + H]⁺). Anal. calc. for C₂₈H₃₅N₃O₆S₂ (573.7): C 58.62, H 6.15, N 7.32; found: C 58.44, H 6.22, N 7.08.

N,N-Bis[2-[(4-methylphenyl)sulfonyl]amino]ethyl]-L-tyrosine Methyl Ester (**9**). Yellow waxy solid (10.6 g, 90%). ¹H-NMR: 7.71, 7.30 (*AA'BB'*, *J* = 8.1, 8 H); 7.08, 6.85 (*AA'BB'*, *J* = 8.4, 4 H); 6.22 (*br. s*, 1 H); 4.66 (*br. s*, 2 H); 3.67 (*s*, 3 H); 3.39 (*dd*, *J* = 9.9, 5.4, 1 H); 2.95 (*dd*, *J* = 14.3, 5.4, 1 H); 2.86–2.57 (*m*, 9 H); 2.41 (*s*, 6 H). ¹³C-NMR: 172.6 (C); 154.8 (C); 143.4 (C); 136.5 (C); 130.2 (CH); 129.7 (CH); 129.6 (C); 127.0 (CH); 115.8 (CH); 64.4 (CH); 51.5 (Me); 50.1 (CH₂); 40.7 (CH₂); 34.4 (CH₂); 21.4 (Me). ESI-MS: 590 ([*M* + H]⁺), 1179 ([2*M* + H]⁺). Anal. calc. for C₂₈H₃₅N₃O₇S₂ (589.7): C 57.03, H 5.98, N 7.13; found: C 56.90, H 6.09, N 6.99.

4. *O*-[4-Methylphenyl)sulfonyl]-N,N-bis[2-[(4-methylphenyl)sulfonyl]amino]ethyl]-L-tyrosine Methyl Ester (**10**). A soln. of **9** (5.30 g, 9.0 mmol) and TsCl (3.20 g, 17 mmol) in pyridine (15 ml) is stirred at r.t. for 1 day. Then more TsCl is added (1.7 g, 9.0 mmol) and the mixture kept stirring for one more day. After addition of 10% aq. Na₂CO₃ soln. (20 ml), the mixture is extracted with AcOEt (3 × 10 ml) and the org. phase dried

(Na₂SO₄), and evaporated: **10** (4.8 g, 72%). Yellow waxy solid, pure enough to be used directly for the following step. ¹H-NMR: 7.72, 7.30 (2 AA'BB', *J* = 8.1, 12 H); 7.14, 6.91 (AA'BB', *J* = 8.5, 4 H); 4.96 (br. s, 2 H); 3.64 (s, 3 H); 3.44 (*t*, *J* = 7.2, 1 H); 3.02–2.60 (*m*, 10 H); 2.46 (s, 6 H); 2.42 (s, 3 H). ¹³C-NMR: 172.4 (C); 147.4 (C); 143.3 (C); 142.4 (C); 138.0 (C); 137.3 (C); 132.2 (C); 130.4 (CH); 129.7 (2 × CH); 128.4 (CH); 127.0 (CH); 122.5 (CH); 64.7 (CH); 51.6 (Me); 50.7 (CH₂); 40.9 (CH₂); 34.8 (CH₂); 21.4 (2 Me). ESI-MS: 744 ([*M* + H]⁺). Anal. calc. for C₃₅H₄₁N₃O₉S₂ (743.9): C 56.51, H 5.56, N 5.65; found: C 56.60, H 5.71, N 5.49.

5. *O*-[(*tert*-Butyl)dimethylsilyl]-*N,N*-bis[2-[(4-methylphenyl)sulfonyl]amino]ethyl]-*L*-tyrosine Methyl Ester (**11**). To a soln. of **9** (15 g, 26.0 mmol) and (*tert*-butyl)dimethylsilyl chloride (5.8 g, 38.0 mmol) in MeCN (100 ml) containing 4-Å-molecular sieves, ¹Pr₂EtN (9.86 g, 76.4 mmol) is slowly added and the mixture refluxed for 1 h under N₂. The mixture is filtered, the filtrate evaporated, and the residue rinsed with H₂O and extracted with AcOEt (3 × 30 ml). The org. phase is dried (Na₂SO₄) and evaporated: **11** (17.0 g, 93%). Yellow waxy solid, pure enough to be used for the following step. ¹H-NMR: 7.74, 7.28 (AA'BB', *J* = 8.2, 8 H); 7.02, 6.77 (AA'BB', *J* = 8.3, 4 H); 5.09 (br. s, 2 H); 3.60 (s, 3 H); 3.38 (*t*, *J* = 7.7, 1 H); 2.89–2.59 (*m*, 10 H); 2.41 (s, 6 H); 1.00 (s, 9 H); 0.09 (s, 6 H). ¹³C-NMR: 172.9 (C); 154.6 (C); 143.6 (C); 137.3 (C); 131.0 (C); 130.5 (CH); 130.1 (CH); 127.5 (CH); 120.5 (CH); 65.2 (CH); 51.8 (Me); 51.1 (CH₂); 41.4 (CH₂); 35.5 (CH₂); 26.1 (Me); 21.9 (Me); 18.2 (C); –3.2 (Me). ESI-MS: 704 ([*M* + H]⁺). Anal. calc. for C₃₄H₄₉N₃O₇S₂Si (704.0): C 58.01, H 7.02, N 5.97; found: C 57.78, H 7.05, N 6.02.

6. *Macrocyclization Reaction with 2,6-Bis(chloromethyl)pyridine: General Procedure.* The functionalized diethylenetriamine **8**, **10**, or **11** (10.0 mmol) and 2,6-bis(chloromethyl)pyridine (10.0 mmol) are dissolved in MeCN (60 ml), and anh. K₂CO₃ (40.0 mmol) is added. The mixture is vigorously stirred and refluxed for 6 h. The solvent is evaporated, the residue washed with H₂O and extracted with AcOEt (3 × 30 ml), the org. phase dried (Na₂SO₄) and evaporated, and the yellow waxy solid crystallized from AcOEt/hexane.

3,9-Bis[(4-Methylphenyl)sulfonyl]- α -(phenylmethyl)-3,6,9,15-tetraazabicyclo[9.3.1]pentadeca-1(15),11,13-triene-6-acetic Acid Methyl Ester (**12**): White solid (4.4 g, 65%). M.p. 152–154° (AcOEt/hexane). ¹H-NMR: 7.76 (*t*, *J* = 7.7, 1 H); 7.70 (1/2 AA'BB', *J* = 8.2, 4 H); 7.39–7.13 (*m*, 11 H); 4.28 (*d*, *J* = 12.1, 2 H); 4.23 (*d*, *J* = 12.1, 2 H); 3.58 (s, 3 H); 3.48 (*dd*, *J* = 8.8, 6.7, 1 H); 3.08–2.87 (*m*, 5 H); 2.72 (*dd*, *J* = 14.1, 8.8, 1 H); 2.47 (s, 6 H); 2.37–2.22 (*m*, 4 H). ¹³C-NMR: 174.2 (C); 155.3 (C); 144.0 (C); 139.3 (CH); 138.6 (C); 135.9 (C); 130.2 (CH); 129.4 (CH); 128.6 (CH); 127.6 (CH); 126.7 (CH); 124.8 (CH); 68.0 (CH); 55.0 (CH₂); 53.1 (CH₂); 51.9 (Me); 46.2 (CH₂); 37.3 (CH₂); 22.0 (Me). ESI-MS: 677 ([*M* + H]⁺). Anal. calc. for C₃₅H₄₀N₄O₆S₂ (676.8): C 62.11, H 5.96, N 8.28; found: C 61.97, H 5.99, N 8.28.

3,9-Bis[(4-methylphenyl)sulfonyl]- α -[4-[(4-methylphenyl)sulfonyl]oxy]phenylmethyl]-3,6,9,15-tetraazabicyclo[9.3.1]pentadeca-1(15),11,13-triene-6-acetic Acid Methyl Ester (**13**): White solid (5.1 g, 60%). M.p. 165–167° (AcOEt/hexane). ¹H-NMR: 7.71 (*t*, *J* = 7.8, 1 H); 7.66, 7.32 (AA'BB', *J* = 7.8, 12 H); 7.27 (*d*, *J* = 7.8, 2 H); 7.03, 6.84 (AA'BB', *J* = 8.4, 4 H); 4.26 (*d*, *J* = 12.4, 2 H); 4.19 (*d*, *J* = 12.4, 2 H); 3.53 (s, 3 H); 3.37 (*dd*, *J* = 8.4, 6.6, 1 H); 3.07–2.83 (*m*, 5 H); 2.67 (*dd*, *J* = 14.6, 8.4, 1 H); 2.42 (s, 9 H); 2.40–2.21 (*m*, 4 H). ¹³C-NMR: 173.4 (C); 154.9 (C); 148.1 (C); 145.3 (C); 143.6 (C); 138.8 (CH); 137.3 (C); 135.6 (C); 132.4 (C); 130.1 (CH); 129.9 (CH); 129.8 (CH); 128.5 (CH); 127.1 (CH); 124.2 (CH); 122.1 (CH); 67.5 (CH); 54.6 (CH₂); 52.7 (CH₂); 51.5 (CH₂); 45.9 (CH₂); 36.2 (CH₂); 21.7 (Me); 21.5 (Me). ESI-MS: 847 ([*M* + H]⁺). Anal. calc. for C₄₂H₄₆N₄O₆S₃ (847.0): C 59.56, H 5.47, N 6.61; found: C 59.65, H 5.61, N 6.48.

α -[4-[(*tert*-Butyl)dimethylsilyl]oxy]phenylmethyl]-3,9-bis[(4-methylphenyl)sulfonyl]-3,6,9,15-tetraazabicyclo[9.3.1]pentadeca-1(15),11,13-triene-6-acetic Acid Methyl Ester (**14**): White solid (5.0 g, 62%). M.p. 200–202° (AcOEt/hexane). ¹H-NMR: 7.77 (*t*, *J* = 7.7, 1 H); 7.70, 7.35 (AA'BB', *J* = 8.1, 8 H); 7.38 (*d*, *J* = 7.7, 2 H); 6.99, 6.73 (AA'BB', *J* = 8.3, 4 H); 4.28 (*d*, *J* = 12.0, 2 H); 4.21 (*d*, *J* = 12.0, 2 H); 3.56 (s, 3 H); 3.41 (*dd*, *J* = 8.5, 7.1, 1 H); 3.02–2.89 (*m*, 5 H); 2.97 (*dd*, *J* = 16.3, 7.1, 1 H); 2.45 (s, 6 H); 2.38–2.30 (*m*, 4 H); 0.99 (s, 9 H); 0.19 (s, 6 H). ¹³C-NMR: 174.3 (C); 155.3 (C); 154.4 (C); 143.9 (C); 139.2 (CH); 135.9 (C); 131.2 (C); 130.3 (CH); 130.2 (CH); 127.6 (CH); 124.8 (CH); 120.3 (CH); 68.1 (CH); 55.0 (CH₂); 53.0 (CH₂); 51.8 (Me); 46.3 (CH₂); 36.6 (CH₂); 26.1 (Me); 22.0 (Me); 18.6 (C); –4.0 (Me). ESI-MS: 807 ([*M* + H]⁺). Anal. calc. for C₄₁H₅₄N₄O₇S₂Si (807.1): C 61.01, H 6.74, N 6.94; found: C 60.88, H 6.91, N 6.90.

7. α -(Phenylmethyl)-3,6,9,15-tetraazabicyclo[9.3.1]pentadeca-1(15),11,13-triene-6-acetic Acid (**15**). A mixture of **12** (3.96 g, 5.87 mmol), 48% aq. HBr soln. (39.6 ml, 352 mmol), AcOH (10.0 ml, 175 mmol), and phenol (3.31 g, 35.2 mmol) is refluxed for 12 h. The soln. is then diluted with H₂O and extracted with CH₂Cl₂ (3 × 20 ml). The aq. phase is evaporated, and the same quantity of reactants is added to the residue; the resulting soln. is refluxed for additional 12 h. The soln. is then extracted with CH₂Cl₂ (3 × 20 ml), the aq. phase concentrated to ca. 2 ml, and Et₂O (15 ml) added. The white-pink crystals obtained are isolated by filtration and washed with acetone: **15** · 2 HBr · 2 H₂O (2.43 g, 75%). White solid. M.p. 125–130°. ¹H-NMR (D₂O): 7.76 (*t*, *J* = 7.8, 1 H); 7.27–7.20 (*m*, 6 H); 7.11 (*tt*, *J* = 7.1, 1.4, 1 H); 4.44 (s, 4 H); 3.85 (*t*, *J* = 7.6, 1 H); 3.15 (*dd*, *J* = 14.2, 7.1,

1 H); 3.01 (*dd*, $J = 14.2, 8.0, 1$ H); 2.96 (*m*, 8 H). $^{13}\text{C-NMR}$ (D_2O): 176.1 (C); 148.9 (C); 140.0 (CH); 138.2 (C); 129.6 (CH); 129.5 (CH); 127.6 (CH); 122.6 (CH); 69.2 (CH); 51.8 (CH_2); 49.9 (CH_2); 46.9 (CH_2); 35.0 (CH_2). ESI-MS: 355 ($[\text{M} + \text{H}]^+$), $\text{C}_{20}\text{H}_{26}\text{N}_4\text{O}_2^+$; calc. 354.4). Anal. calc. for $\text{C}_{20}\text{H}_{26}\text{N}_4\text{O}_2 \cdot 2 \text{HBr} \cdot 2 \text{H}_2\text{O}$ (552.3): C 43.49, H 5.84, N 10.14; found: C 43.37, H 5.85, N 9.96.

α -[4-[(4-Methylphenyl)sulfonyloxy]phenyl]methyl]-3,6,9,15-tetraazabicyclo[9.3.1]pentadeca-1(15),11,13-triene-6-acetic Acid (**16**). As described for **15**, **13** (1.69 g, 2.00 mmol): **16** · 2 HBr (0.95 g, 69%). Amorphous powder. $^1\text{H-NMR}$ (D_2O): 7.73 (*t*, $J = 7.8, 1$ H); 7.42 (1/2 *AA'BB'*, $J = 7.8, 2$ H); 7.23–7.05 (*m*, 6 H); 6.65 (1/2 *AA'BB'*, $J = 8.2, 2$ H); 4.38 (*s*, 4 H); 3.72 (*t*, $J = 7.6, 1$ H); 3.05 (*dd*, $J = 13.7, 6.7, 1$ H); 3.03–2.75 (*m*, 9 H); 2.16 (*s*, 3 H). ESI-MS: 525 ($[\text{M} + \text{H}]^+$), $\text{C}_{27}\text{H}_{32}\text{N}_4\text{O}_5\text{S}^+$; calc. 524.6). Anal. calc. for $\text{C}_{27}\text{H}_{32}\text{N}_4\text{O}_5\text{S} \cdot 2 \text{HBr}$ (686.5): C 47.24, H 4.99, N 8.16; found: C 46.98, H 5.09, N 8.03.

8. α -[4-(4-Hydroxyphenyl)methyl]-3,6,9,15-tetraazabicyclo[9.3.1]pentadeca-1(15),11,13-triene-6-acetic Acid Methyl Ester (**17**). A soln. of **14** (2.20 g, 2.73 mmol), 33% HBr in AcOH (30 ml), and phenol (1.54 g, 16.4 mmol) is heated at 60° for 18 h. H_2O is then added (50 ml), and the mixture is extracted with CH_2Cl_2 (3 × 20 ml). The aq. phase is evaporated: **17** · 2 HBr (1.48 g, 99%). Amorphous solid, which is used for the next reaction without further purification. $^1\text{H-NMR}$ (D_2O): 7.52 (*t*, $J = 7.8, 1$ H); 7.01 (*d*, $J = 7.8, 2$ H); 6.84, 6.41 (*AA'BB'*, $J = 8.4, 4$ H); 4.19 (*s*, 4 H); 3.58 (*t*, $J = 7.6, 1$ H); 3.29 (*s*, 3 H); 2.77–2.60 (*m*, 10 H). $^{13}\text{C-NMR}$ (D_2O): 170.5 (C); 149.7 (C); 149.5 (C); 140.7 (CH); 131.3 (CH); 131.0 (C); 123.3 (CH); 116.8 (CH); 69.8 (CH); 53.4 (Me); 52.3 (CH_2); 49.6 (CH_2); 47.5 (CH_2); 34.9 (CH_2). ESI-MS: 385 ($[\text{M} + \text{H}]^+$), $\text{C}_{21}\text{H}_{28}\text{N}_4\text{O}_3^+$; calc. 384.5). Anal. calc. for $\text{C}_{21}\text{H}_{28}\text{N}_4\text{O}_3 \cdot 2 \text{HBr}$ (546.3): C 46.17, H 5.54, N 10.26; found: C 45.89, H 5.69, N 10.12.

9. α^6 -(Phenylmethyl)-3,6,9,15-tetraazabicyclo[9.3.1]pentadeca-1(15),11,13-triene-3,6,9-triacetic Acid (**1**). To a soln. of **15** (0.50 g, 0.91 mmol) and chloroacetic acid (0.215 g, 2.28 mmol) in H_2O (1 ml), 6*M* aq. KOH (0.5 ml) and 2 drops of a phenolphthalein soln. (0.2% in MeOH) are added. The soln. is heated at 80° for 6 h, maintaining pH 10 (persistent pink color of phenolphthalein) by slow addition of KOH soln. The soln. is then acidified with aq. 2*N* HCl and concentrated to a small volume. The residue is purified by column chromatography (*XAD 1600*, $\text{H}_2\text{O} \rightarrow \text{H}_2\text{O}/\text{MeOH}$ 7:3): pure **1** (0.29 g, 68%). White amorphous solid. $^1\text{H-NMR}$ (D_2O): 7.76 (*t*, $J = 7.8, 1$ H); 7.47 (*d*, $J = 7.8, 2$ H); 7.26–7.06 (*m*, 5 H); 4.52 (*s*, 4 H); 3.77 (*m*, 5 H); 3.37–3.13 (*m*, 4 H); 2.99–2.70 (*m*, 6 H). $^{13}\text{C-NMR}$ (D_2O): 177.8 (C); 176.2 (C); 150.6 (C); 141.3 (CH); 138.6 (C); 130.5 (CH); 130.1 (CH); 128.2 (CH); 124.2 (CH); 67.4 (CH); 60.6 (CH_2); 57.6 (CH_2); 54.6 (CH_2); 49.1 (CH_2); 35.2 (CH_2). MALDI-MS: 471 ($[\text{M} + \text{H}]^+$), 493 ($[\text{M} + \text{Na}]^+$), 509 ($[\text{M} + \text{K}]^+$). Anal. calc. for $\text{C}_{24}\text{H}_{30}\text{N}_4\text{O}_6$ (470.5): C 61.26, H 6.43, N 11.91; found: C 61.25, H 6.60, N 12.01.

10. α -(Phenylmethyl)-3,6-bis(phosphonomethyl)-3,6,9,15-tetraazabicyclo[9.3.1]pentadeca-1(15),11,13-triene-6-acetic Acid (**2**). A soln. of **15** (0.15 g, 0.27 mmol) in 6*M* HCl (5 ml) and phosphorous acid (0.114 g, 1.39 mmol) is brought to reflux, and paraformaldehyde (0.1 g, 3.30 mmol) is portionwise added within ca. 1 h. At the end of the addition, the soln. is refluxed for further 8 h. The mixture is concentrated to ca. 1 ml, and EtOH is added to precipitate **2**, which is filtered, washed with EtOH and then with Et_2O and finally dried: **2** (0.096 g, 61%). White amorphous solid. $^1\text{H-NMR}$ (D_2O): 7.77 (*t*, $J = 7.8, 1$ H); 7.27 (*d*, $J = 7.8, 2$ H); 7.16 (*m*, 4 H); 7.10 (*m*, 1 H); 4.77 (*m*, 4 H); 3.75 (*t*, $J = 8.1, 1$ H); 3.59–3.40 (*m*, 6 H); 3.42 (*d*, $J = 11.8, 4$ H); 3.13–2.94 (*m*, 4 H). $^{13}\text{C-NMR}$ (D_2O): 174.4 (C); 148.5 (CH); 139.4 (CH); 136.7 (C); 128.6 (CH); 128.2 (CH); 126.3 (C); 122.1 (CH); 65.0 (CH); 58.7 (CH_2); 54.1 (CH_2); 51.0 (*d*, $J(\text{C,P}) = 138, \text{CH}_2$); 46.4 (CH_2); 33.0 (CH_2). MALDI-MS: 581 ($[\text{M} + \text{K}]^+$), 565 ($[\text{M} + \text{Na}]^+$), 543 ($[\text{M} + \text{H}]^+$), $\text{C}_{22}\text{H}_{32}\text{N}_4\text{O}_8\text{P}_2^+$; calc. 542.5). Anal. calc. for $\text{C}_{22}\text{H}_{32}\text{N}_4\text{O}_8\text{P}_2 \cdot 2 \text{H}_2\text{O}$ (578.5): C 45.68, H 6.27, N 9.68; found: C 45.39, H 6.39, N 9.50.

11. α^6 -[3-Carboxy-4-(2-methoxy-2-oxoethoxy)phenyl]methyl]-3,6,9,15-tetraazabicyclo[9.3.1]pentadeca-1(15),11,13-triene-3,6,9-triacetic Acid Trimethyl Ester (**18**). A mixture of **17** (0.250 g, 0.46 mmol), silver carbonate (0.758 g, 2.75 mmol), and methyl bromoacetate (260 μl , 2.75 mmol) in MeCN (2 ml) is vigorously stirred for 2 h in the dark. The mixture is then filtered and the soln. obtained is evaporated. The crude product is purified by FC (silica gel, $\text{CH}_2\text{Cl}_2/\text{MeOH}/\text{NH}_3$ 95:5:0.1): **18** (0.172 g, 58%). $^1\text{H-NMR}$: 7.71 (*m*, 2 H); 7.37–7.27 (*m*, 2 H); 7.00 (*m*, 1 H); 6.75 (*m*, 1 H); 4.37 (*d*, $J = 12.0, 2$ H); 4.23 (*d*, 12.0, 2 H); 3.96 (*s*, 2 H); 3.75 (*s*, 6 H); 3.70 (*s*, 3 H); 3.55 (*s*, 4 H); 3.53 (*s*, 3 H); 3.21 (*t*, $J = 6.4, 1$ H); 2.92 (*dd*, $J = 14.5, 6.4, 1$ H); 2.75–2.29 (*m*, 9 H). $^{13}\text{C-NMR}$: 173.4 (C); 169.7 (C); 169.0 (C); 168.1 (C); 156.2 (C); 155.1 (C); 138.2 (CH); 130.5 (C); 130.2 (CH); 130.1 (CH); 123.0 (CH); 114.5 (CH); 113.9 (C); 70.4 (CH_2); 65.2 (CH_2); 61.5 (CH_2); 52.1 (Me); 52.0 (Me); 51.8 (CH); 51.3 (Me); 49.2 (CH_2); 47.5 (CH_2); 29.6 (CH_2). MALDI-MS: 645 ($[\text{M} + \text{H}]^+$), 667 ($[\text{M} + \text{Na}]^+$), 683 ($[\text{M} + \text{K}]^+$). Anal. calc. for $\text{C}_{31}\text{H}_{40}\text{N}_4\text{O}_{11}$ (644.7): C 57.76, H 6.25, N 8.69; found: C 57.53, H 6.41, N 8.77.

12. α^6 -[3-Carboxy-4-(carboxymethoxy)phenyl]methyl]-3,6,9,15-tetraazabicyclo[9.3.1]pentadeca-1(15),11,13-triene-3,6,9-triacetic Acid (**3**). A soln. of **18** (0.110 g, 0.171 mmol) and KOH (0.400 g, 0.700 mmol) in MeOH (5 ml) is vigorously stirred and heated at 60° for 4 h. The solvent is then evaporated and the solid obtained is washed thoroughly with $\text{MeOH}/\text{Et}_2\text{O}$: **3** (0.059 g). White amorphous solid. $^1\text{H-NMR}$ (D_2O): 7.69 (*t*, $J = 7.5,$

1 H); 7.23 (m, 2 H); 6.95 (m, 2 H); 6.65 (d, $J = 8.0$, 1 H); 4.28–4.12 (m, 6 H); 3.81 (m, 1 H); 3.49 (s, 4 H); 3.25–2.95 (m, 6 H); 2.79–2.52 (m, 4 H). ^{13}C -NMR (D_2O): 177.6 (C); 176.8 (C); 176.7 (C); 173.4 (C); 157.2 (C); 156.9 (C); 139.7 (CH); 131.9 (C); 130.8 (CH); 130.7 (2 CH); 115.4 (CH); 115.2 (C); 81.6 (CH); 70.4 (CH_2); 67.8 (CH_2); 65.1 (CH_2); 59.2 (CH_2); 54.5 (CH_2); 51.0 (CH_2). MALDI-MS: 589 ($[M + \text{H}]^+$, $\text{C}_{27}\text{H}_{32}\text{N}_4\text{O}_{11}^+$; calc. 588.6), 611 ($[M + \text{Na}]^+$), 627 ($[M + \text{K}]^+$).

13. *Water Proton Relaxivity Measurements*. The longitudinal H_2O proton relaxation rate was measured with a *Stelar-Spinmaster* spectrometer (*Stelar*, Mede, Pavia, Italy) operating at 20 MHz, by means of the standard inversion-recovery technique (16 experiments, 2 scans). A typical 90° pulse width was 3.5 μs and the reproducibility of the T_1 data was $\pm 0.5\%$. The temp. was controlled with a *Stelar-VTC-91* air-flow heater equipped with a copper-constantan thermocouple (uncertainty $\pm 0.1^\circ$). The proton $1/T_1$ NMRD profiles were measured over a continuum of magnetic-field strength from 0.00024 to 0.28 T (corresponding to 0.01–12 MHz proton Larmor frequency) on a *Stelar-Fast-Field-Cycling* relaxometer. This relaxometer works under complete computer control with an absolute uncertainty in $1/T_1$ of $\pm 1\%$. Data points at 20 MHz, were added to the experimental NMRD profiles and were recorded on the *Stelar Spinmaster* (20 MHz). The concentration of the Gd^{III} complexes in the solutions used for the relaxometric determinations was obtained by means of ICP analysis.

14. *^{17}O -NMR Measurements*. Variable-temperature ^{17}O -NMR measurements were recorded at 2.1 T by means of the *Jeol EX-90* and at 7.05 T by means of the *Bruker Avance-300* spectrometer, equipped with a 5-mm probe, by using a D_2O external lock. Experimental settings were: spectral width 10000 Hz, 90° pulse (7 μs), acquisition time 10 ms, 1000 scans, and without sample spinning. Aq. solns. containing 2.6% of ^{17}O isotope (*Yeda*, Israel) were used. The observed transverse relaxation rates ($R_{2\text{obs}}^0$) were calculated from the signal width at half-height ($\Delta\nu_{1/2}$): $R_{2\text{obs}}^0 = \pi \Delta\nu_{1/2}$.

Financial support from *Bracco Imaging S.p.a.*, Milan, and from *Italian CNR* (Target Project on Biotechnology) is gratefully acknowledged. Two of the authors (C. C. and M. S.) are thankful to the Dipartimento di Chimica Organica e Industriale, Università degli Studi, Milan, Italy, for kind hospitality in their laboratories.

REFERENCES

- [1] B. L. Engelstad, G. L. Wolf, in 'Magnetic Resonance Imaging', Eds. D. D. Stark and W. G. Bradley Jr., Mosby, St Louis, pp. 161–181, 1988.
- [2] P. A. Rinck, 'Magnetic Resonance in Medicine', Blackwell Scientific Publications, Oxford, 1993.
- [3] P. Caravan, J. J. Ellison, T. J. McMurry, R. B. Lauffer, *Chem. Rev.* **1999**, *99*, 2293.
- [4] 'The Chemistry of Contrast Agents in Medical Magnetic Resonance Imaging', Eds. A. E. Merbach and E. Toth, John Wiley & Sons, Ltd., Chichester, 2001.
- [5] R. B. Lauffer, *Chem. Rev.* **1987**, *87*, 901.
- [6] S. Aime, M. Botta, M. Fasano, E. Terreno, *Chem. Soc. Rev.* **1998**, *27*, 19.
- [7] E. Toth, O. M. Ni Dhubhghaill, G. Besson, L. Helm, A. E. Merbach, *Magn. Reson. Chem.* **1999**, *37*, 701.
- [8] D. H. Powell, O. M. Ni Dhubhghaill, D. Pubanz, L. Helm, Y. S. Lebedev, W. Schlaepfer, A. E. Merbach, *J. Am. Chem. Soc.* **1996**, *118*, 9333.
- [9] S. Aime, M. Botta, S. Geninatti Crich, G. B. Giovenzana, R. Pagliarin, M. Sisti, E. Terreno, *Magn. Reson. Chem.* **1998**, *36*, S200.
- [10] S. Aime, E. Gianolio, E. Terreno, G. B. Giovenzana, R. Pagliarin, M. Sisti, G. Palmisano, M. Botta, M. P. Lowe, D. Parker, *J. Biol. Inorg. Chem.* **2000**, *5*, 488.
- [11] J. Xu, S. J. Franklin Jr., D. W. Whisenhunt, K. N. Raymond, *J. Am. Chem. Soc.* **1995**, *117*, 7245.
- [12] S. Hajela, M. Botta, S. Giraud, J. Xu, K. N. Raymond, S. Aime, *J. Am. Chem. Soc.* **2000**, *122*, 11228.
- [13] D. M. J. Doble, M. Botta, J. Wang, S. Aime, A. Barge, K. N. Raymond, *J. Am. Chem. Soc.* **2001**, *123*, 10758.
- [14] W. D. Kim, G. E. Kiefer, F. Maton, K. McMillan, R. N. Muller, A. D. Sherry, *Inorg. Chem.* **1995**, *34*, 2233.
- [15] S. Aime, M. Botta, S. Geninatti Crich, G. B. Giovenzana, G. Jommi, R. Pagliarin, M. Sisti, *Inorg. Chem.* **1997**, *36*, 2992.
- [16] S. Aime, M. Botta, S. Geninatti Crich, G. B. Giovenzana, G. Jommi, R. Pagliarin, M. Sisti, *J. Chem. Soc., Chem. Commun.* **1995**, 1885.
- [17] S. Aime, M. Botta, L. Frullano, S. Geninatti Crich, G. B. Giovenzana, R. Pagliarin, G. Palmisano, F. Riccardi Sirtori, M. Sisti, *J. Med. Chem.* **2000**, *43*, 4017.
- [18] L. Banci, I. Bertini, C. Luchinat, 'Nuclear and Electron Relaxation', VCH, Weinheim, 1991.

- [19] I. Solomon, N. Bloembergen, *J. Chem. Phys.* **1956**, 25, 261.
- [20] N. Bloembergen, L. O. Morgan, *J. Chem. Phys.* **1961**, 34, 842.
- [21] M. Botta, *Eur. J. Inorg. Chem.* **2000**, 399.
- [22] K. Mickei, L. Helm, E. Brucher, A. E. Merbach, *Inorg. Chem.* **1993**, 32, 3844.
- [23] T. J. Swift, R. E. J. Connick, *J. Chem. Phys.* **1962**, 37, 307.
- [24] D. H. Powell, M. Favre, N. Graeppli, O. M. Ni Dhubhghaill, D. Pubanz, A. E. Merbach, *J. Alloys Compd.* **1995**, 225, 246.
- [25] G. Gonzalez, D. H. Powell, V. Tissieres, A. E. Merbach, *J. Chem. Phys.* **1994**, 98, 53.
- [26] C. A. Chang, H. G. Brittain, J. Telser, M. F. Tweedle, *Inorg. Chem.* **1990**, 29, 4468.
- [27] L. Burai, V. Hietapelto, R. Kiraly, E. Toth, E. Brucher, *Magn. Reson. Med.* **1997**, 38, 146.
- [28] S. Aime, M. Botta, M. Fasano, S. Geninatti Crich, E. Terreno, *J. Biol. Inorg. Chem.* **1996**, 1, 312.
- [29] S. Aime, M. Chiaussa, G. Digilio, E. Gianolio, E. Terreno, *J. Biol. Inorg. Chem.* **1999**, 4, 766.
- [30] S. Aime, M. Botta, S. Geninatti Crich, G. B. Giovenzana, R. Pagliarin, R. Piccinini, M. Sisti, E. Terreno, *J. Biol. Inorg. Chem.* **1997**, 2, 470.
- [31] S. Aime, M. Botta, F. Fedeli, E. Gianolio, E. Terreno, P. L. Anelli, *Chem.–Eur. J.* **2001**, 7, 5261.

Received July 16, 2002